# CHISEL POINT DEV 995 1069 PR – EUTECTOID TO HYPEREUTECTOID STEEL – EARLY MEDIEVAL TIMES – SWITZERLAND

| | |
|---|---|
| **Artefact name** | Chisel point DEV 995 1069 PR |
| **Authors** | Marianne. Senn (EMPA, Dübendorf, Zurich, Switzerland) & Christian. Degrigny (HE-Arc CR, Neuchâtel, Neuchâtel, Switzerland) |
| **Url** | /artefacts/530/ |

## The object

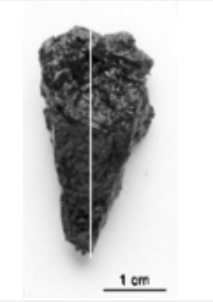


*Credit HE-Arc CR.*

Fig. 1: Chisel point (after Eschenlohr et al. 2007, 275, 314-315),

## Description and visual observation

| | |
|---|---|
| **Description of the artefact** | The rectangular section of a massive moil chisel fragment with an incomplete tip and missing shaft (Fig. 1). Dimensions: L = 3.7cm; WT = 16g. |
| **Type of artefact** | Tool |
| **Origin** | Settlement Develier, Courtételle, Jura, Switzerland |
| **Recovering date** | Excavated in 1995, farm 2 and workshop area 1 |
| **Chronology category** | Early medieval times |
| **chronology tpq** | 550 A.D. |
| **chronology taq** | 650 A.D. |
| **Chronology comment** | |
| **Burial conditions / environment** | Soil |
| **Artefact location** | Office de la Culture, Porrentruy, Jura |
| **Owner** | Office de la Culture, Porrentruy, Jura |
| **Inv. number** | DEV 995/1069 PR |

| | |
|---|---|
| **Recorded conservation data** | Conserved between 1995 and 2000: desiccation at 80°C, mechanical cleaning, passivation with tannic acid and surface protection with Paraloid B72® (Eschenlohr et al. 2007, 75). |

**Complementary information**

Nothing to report.

## Study area(s)


*Credit HE-Arc CR.*

Fig. 2: Location of sampling area,

## Binocular observation and representation of the corrosion structure

Stratigraphic representation: none.

## MiCorr stratigraphy(ies) – Bi

## Sample(s)

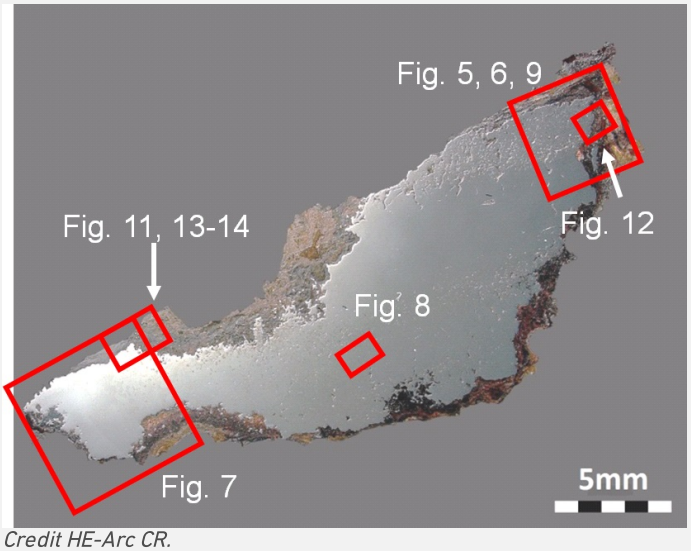


*Credit HE-Arc CR.*

Fig. 3: Micrograph of the cross-section of the chisel point showing the location of Figs. 5 to 9 and 11 to 14,

| | |
|---|---|
| **Description of sample** | A longitudinal cut from a chisel point (Figs. 2 and 3) undertaken after restoration. Dimensions: L = 30mm; W = 11mm (approximately). |
| **Alloy** | Eutectoid to hypereutectoid steel |
| **Technology** | Quench hardened |
| **Lab number of sample** | DEV1069 |
| **Sample location** | Empa (Marianne Senn) |
| **Responsible institution** | Office de la Culture, Porrentruy, Jura |
| **Date and aim of sampling** | 2000, metallography and chemical composition of the metal |

**Complementary information**

Nothing to report.

## Analyses and results

***Analyses performed:***
Metallography (nital etched), Vickers hardness testing, LA-ICP-MS, SEM/EDX.

## Non invasive analysis

## Metal

The remaining metal is a eutectoid to hypereutectoid steel (C 0.8-1 mass%) with cracks and porosity (Figs. 5 and 6). Its composition is given in Table 1 (except Fe). Of the trace elements, only Ni reaches a medium concentration (Ni 0.07 mass%). The composition and the high Ni/Co ratio are atypical for iron worked in smithies of the settlement at Develier-Courtételle JU, CH. The few slag inclusions and their chemical composition confirm this (Table 2). The slag is rich in CaO whereas the pisolithic or bean ore worked in the Central Jura smelting district is rich in $Al_2O_3$. The slag inclusions cannot be smithing slag because the artefact is formed from one piece of metal. The slag probably incorporated while refining the bloom or during the bloom smelting process. The ore from which this metal was smelted cannot yet be identified. Intergranular corrosion has developed, penetrating into the metal structure (Fig. 6). The etched metal shows a dominant martensitic structure, typical of quench hardened steel (Figs. 5, 7, 8 and 9). The characteristic forms of the martensite are non-organised needles (Fig. 8). In restricted areas bainite nodules occur (Figs. 7 and 8). In the centre of the point, hypereutectoid steel is composed of cementite in the grain boundaries and in needle like shapes within the grains (Fig. 10). Hypereutectoid regions also occur in the centre of the shaft and on its left surface (Fig. 5). Here the hypereutectoid steel is composed of martensite and cementite in the grain boundaries and in needle form within the grains (Figs. 6 and 9). Nevertheless, most of the chisel is dominated by eutectoid steel. The average hardness of the quench hardened eutectoid steel is about HV1 690. In the bainite nodules the average hardness drops to about HV1 350, the martensite has an average hardness of HV1 750.

| Elements | V | Cr | Mn | P | Co | Ni | Cu | As | Ag | Ni/Co | C* mass% |
|---|---|---|---|---|---|---|---|---|---|---|---|
| Median mg/kg | 2 | 20 | 2 | 300 | 40 | 680 | 100 | 190 | < | 17 | 0.8-1 |
| Detection limit mg/kg | 1 | 8 | 1 | 70 | 1 | 1 | 1 | 3 | 0.2 | 1 | 6 |
| RSD % | 50 | 36 | 15 | 21 | 5 | 13 | 55 | 10 | - | | |

*visually estimated

Table 1: Chemical composition of the metal. Method of analysis: LA-ICP-MS, Laboratory of Analytical Chemistry, Empa (for details see Devos et al. 2000).

| Structure | Location | $Na_2O$ | MgO | $Al_2O_3$ | $SiO_2$ | $K_2O$ | CaO | $TiO_2$ | FeO | Total | $SiO_2/Al_2O_3$ |
|---|---|---|---|---|---|---|---|---|---|---|---|
| Glass and? | Tip | 0.6 | 2.4 | 7.8 | 50 | 3.9 | 15 | < | 20 | 100 | 6.4 |
| Glass and? | Tip | 0.6 | 2.5 | 8.9 | 65 | 4.7 | 18 | 0.7 | 4.2 | 104 | 7.3 |
| Glass with needles | Middle | 0.7 | 2.6 | 10 | 59 | 4.6 | 21 | 0.7 | 2.5 | 101 | 5.9 |
| Glass with needles | Middle | 0.7 | 2.5 | 8.7 | 58 | 4.7 | 21 | 0.6 | 3.0 | 100 | 6.7 |
| Glass with needles | Middle | 0.8 | 2.3 | 8.5 | 51 | 4.1 | 24 | 0.7 | 3.6 | 95 | 6.0 |

Table 2: Chemical composition of the slag inclusions (mass%). Method of analysis: SEM/EDS, Laboratory of Analytical Chemistry, Empa.

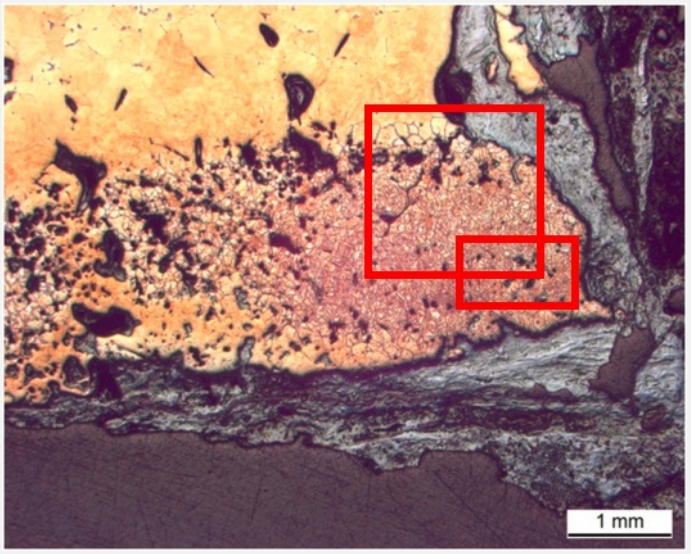


*Credit HE-Arc CR.*

Fig. 5: Micrograph of the metal sample from Fig. 3 (inverted picture, detail), etched, bright field. The metal contains porosity and cracks (in black). The micrographs of Figs. 6 and 9 are marked by the top and bottom rectangles respectively,

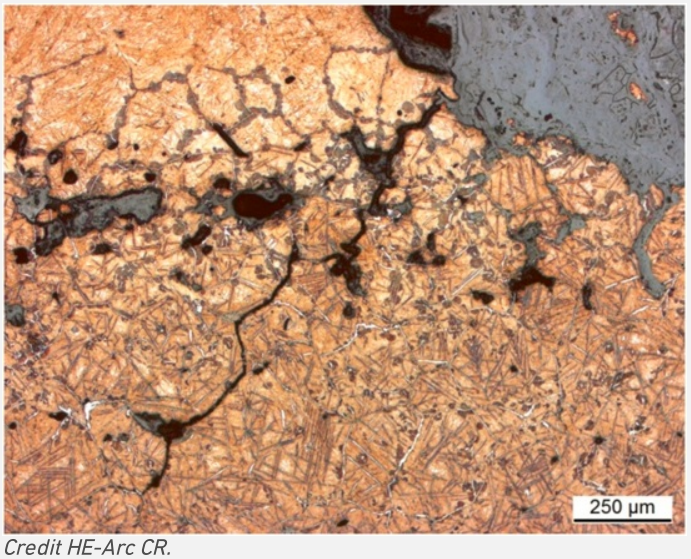


*Credit HE-Arc CR.*

Fig. 6: Micrograph of the metal sample, detail from Fig. 5, etched, bright field. We observe martensite (in orange), cementite (in grey), porosity and intergranular cracks (in black) and corrosion,

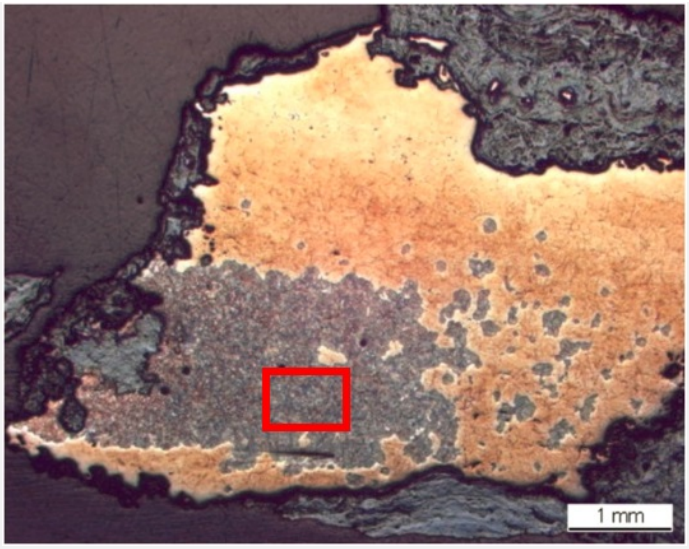


*Credit HE-Arc CR.*

Fig. 7: Micrograph of the metal sample from Fig. 3 (inverted picture, detail), etched, bright field. We observe the metal with martensite (orange) and bainite nodules (blue). The micrograph of Fig. 10 is marked by a rectangle,

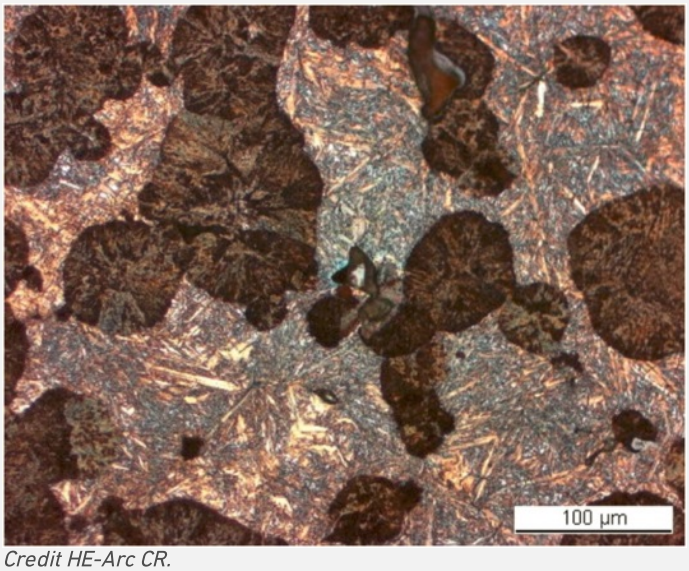


*Credit HE-Arc CR.*

Fig. 8: Micrograph of the metal sample from Fig. 3 (detail), etched, bright field. We observe dark bainite nodules combined with martensite needles,

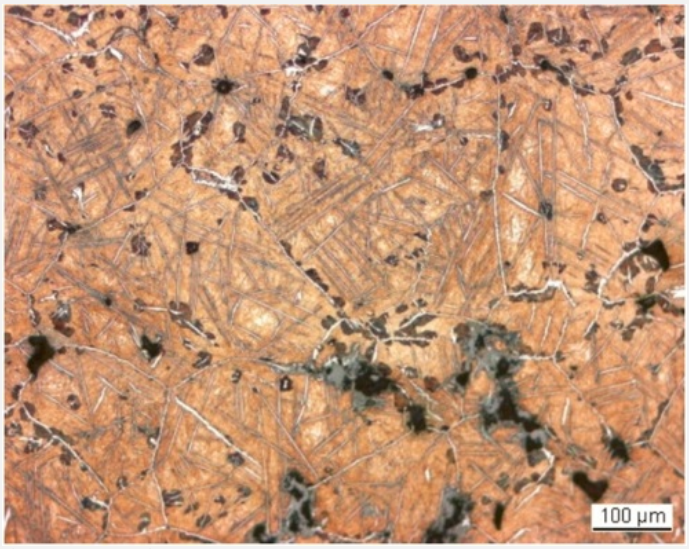


*Credit HE-Arc CR.*

Fig. 9: Micrograph of the metal sample, detail from Fig. 5, etched, bright field. Hypereutectoid steel with a structure of cementite in white in the grain boundaries and in needle form combined with martensite (pink). Some bainite occurs around the grain boundaries,

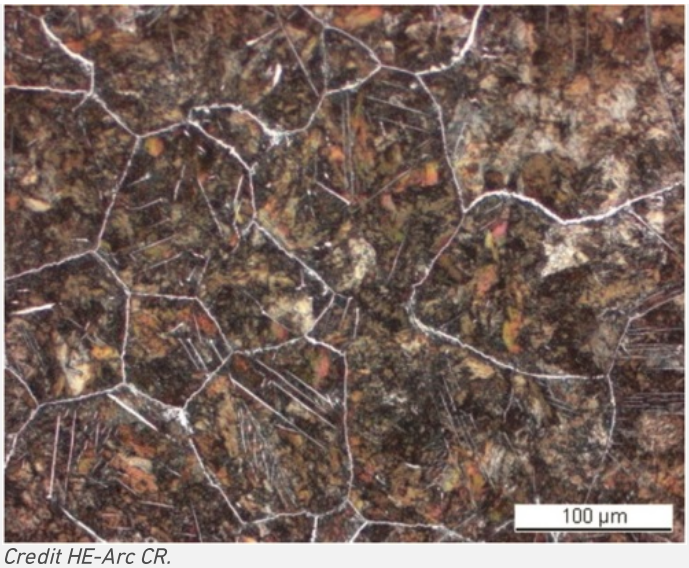


*Credit HE-Arc CR.*

Fig. 10: Micrograph of the metal sample, detail from Fig. 7, etched, bright field. Hypereutectoid steel with a structure of cementite in white in the grain boundaries and in needle form combined with bainite (dark),

| | |
|---|---|
| **Microstructure** | Martensitic structure (non organised needles) + bainite nodules |
| **First metal element** | Fe |
| **Other metal elements** | C |

**Complementary information**

Nothing to report.

## Corrosion layers

The metal is heavily corroded and the thickness of the corrosion crust is irregular, but averages about 0.5mm. The corrosion products enclose different ghost structures: the corrosion crust has preserved the shape of polygonal grains (Figs. 11 and 13) and cementite needles (Fig. 12). Under polarised light, the corrosion products at the metal - corrosion crust interface are dark-red and form an inner S-rich layer (CP3, Figs. 11 and 13). Cl occurs locally (CP3) and C is present in layers CP2 and CP3 (Fig. 13). The outer layer of the corrosion products (CP1) is orange and contains more O than the inner layer CP3 (Figs. 11 and 14).

| Elements | O | S | Cl | Fe | Total |
|---|---|---|---|---|---|
| Inner red/light-grey layer (CP3) | 27 | 1.2 | 1.3 | 72 | 103 |
| Inner dark-red layer (average of 2 similar analyses) (CP2) | 31 | 0.9 | < | 66 | 99 |
| Inner orange grain zone | 36 | < | < | 63 | 101 |
| Outer orange sub-layer (average of 2 similar analyses) (CP1) | 35 | < | < | 63 | 98 |

Table 3: Chemical composition (mass %) of the corrosion crust (from Figs. 11-14). Method of analysis: SEM/EDS, Laboratory of Analytical Chemistry, Empa.

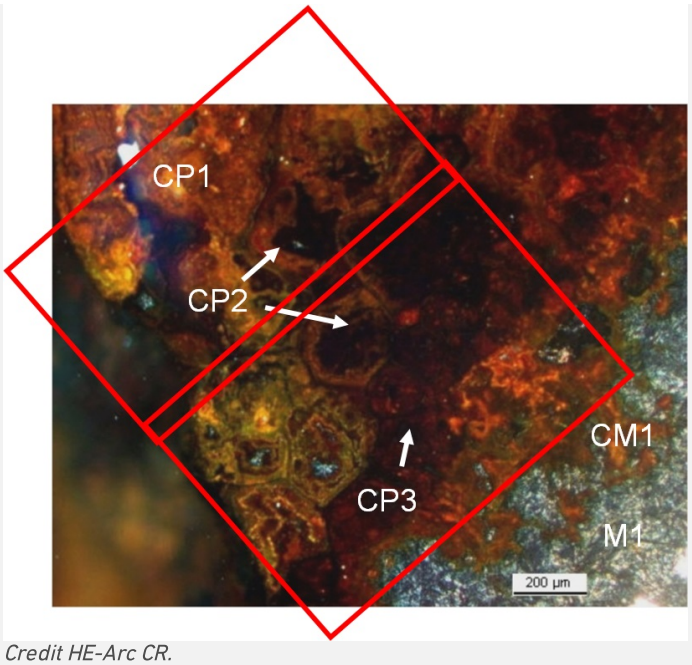


Credit HE-Arc CR.

Fig. 11: Micrograph showing the metal - corrosion crust interface from Fig. 3 (rotated by 270°, detail) and corresponding to the stratigraphy of Fig. 4, unetched, polarised light. Polygonal grains are visible as ghost structure in the corrosion crust. The selected areas for elemental chemical distribution (Figs. 13 and 14) are marked by two rectangles (bottom: Fig. 13 and top: Fig. 14),

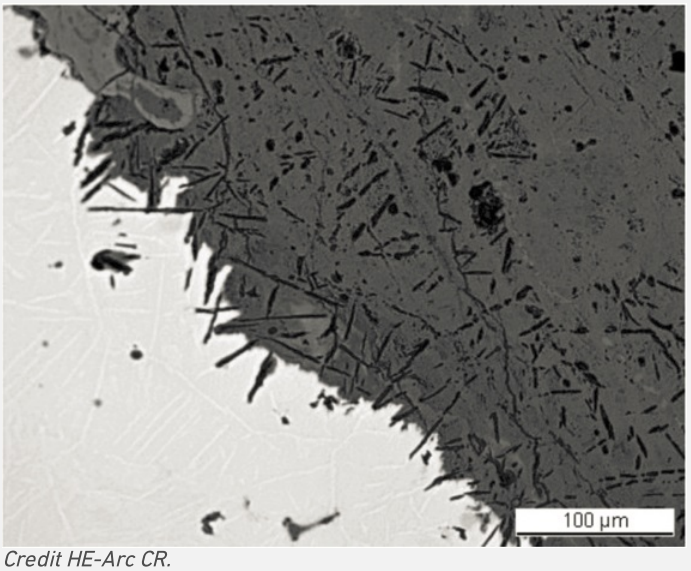


Credit HE-Arc CR.

Fig. 12: Micrograph showing the metal - corrosion crust interface from Fig. 3 (detail), unetched, bright field. The cementite is visible as white needles in the metal and its ghost structure as black needles in the corrosion crust,

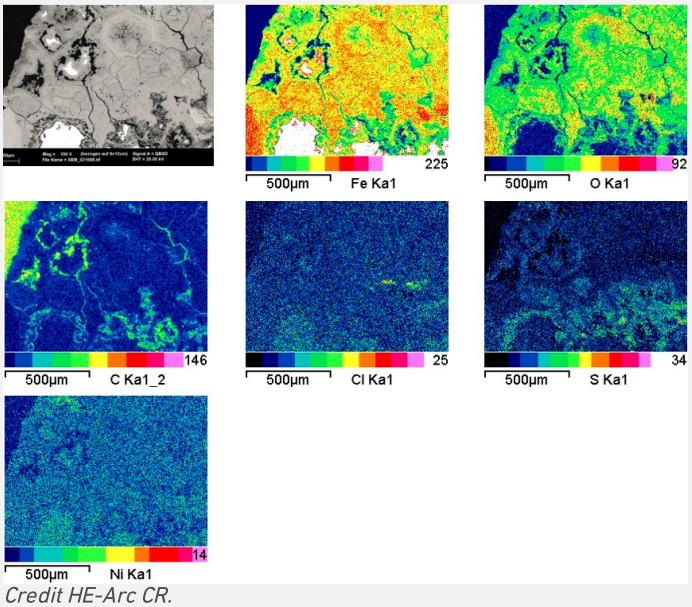


Credit HE-Arc CR.

Fig. 13: SEM image, BSE-mode, and elemental chemical distribution of the selected area from Fig. 11 (rotated by 45°). Method of examination: SEM/EDS, Laboratory of Analytical Chemistry, Empa,

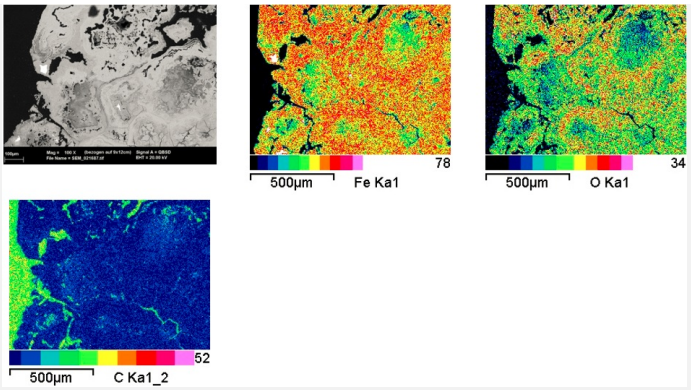


*Credit HE-Arc CR.*

Fig. 14: SEM image, BSE-mode, and elemental chemical distribution of the selected area from Fig. 11 (rotated by 45°). Method of examination: SEM/EDS, Laboratory of Analytical Chemistry, Empa,

| | |
|---|---|
| **Corrosion form** | Uniform - intergranular |
| **Corrosion type** | ? |

**Complementary information**

Nothing to report.

## MiCorr stratigraphy(ies) – CS

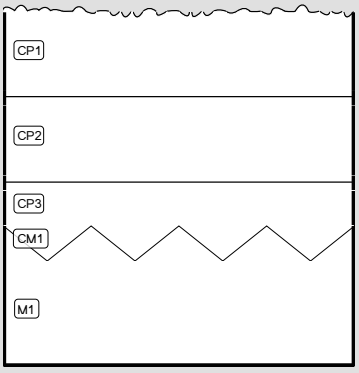


Fig. 4: Stratigraphic representation of the chisel point in cross-section using the MiCorr application. The characteristics of the strata are only accessible by clicking on the drawing that redirects you to the search tool by stratigraphy representation. This representation can be compared to Fig. 11, Credit HE-Arc CR.

## Synthesis of the binocular / cross-section examination of the corrosion structure

Corrected stratigraphic representation: none.

## Conclusion

The tool is made of hard, eutectoid to hypereutectoid steel and was, as a last manufacturing step, entirely quenched. In this state it is too hard and brittle to be used. It is likely that the quenched hypereutectoid structure provoked the breakage of the tool when it was first used. The absence of a tempering process at the end is unclear. The chemical composition of the metal and the slag inclusions indicate that the artefact was imported to the hamlet of Develier-Courtételle JU. The corrosion has, in areas, replaced the metal structure retaining a ghost structure; the outer layer has been mostly removed during surface cleaning. Extensive pitting corrosion has occurred, typical for steel with an elevated C content. The presence of S in the inner layer can be explained by putrefaction processes in the soil. Chlorides are still present at the metal-corrosion interface as no desalination process was attempted. Iron carbonates are present in the centre of a corrosion pit. The corrosion is of terrestrial type.

## References

*References on object and sample*

**References object**

1. Eschenlohr, L., Friedli, V., Robert-Charrue Linder, C., Senn, M. (2007) Develier-Courtételle. Un habitat mérovingien. Métallurgie du fer et mobilier métallique. Cahier d'archéologie jurassienne 14 (Porrentruy), 314-315.

**References sample**

2. Eschenlohr, L., Friedli, V., Robert-Charrue Linder, C., Senn, M. (2007) Develier-Courtételle. Un habitat mérovingien. Métallurgie du fer et mobilier métallique. Cahier d'archéologie jurassienne 14 (Porrentruy), 275.

*References on analytic methods and interpretation*